DC field distribution in XLPE-insulated DC model cable with polarity reversal and thermal gradient

N. Adi, Gilbert Teyssedre, T. T. N. Vu, N. Sinisuka

DC Field Distribution in XLPE-Insulated DC Model Cable with Polarity Inversion and Thermal Gradient

Nugroho Adi[1,2,3*], G. Teyssedre[1], T. T. N. Vu[4], N. I. Sinisuka[2]
[1]LAPLACE, Université de Toulouse, CNRS, INPT, UPS, France, Bat 3R3, 118, route de Narbonne, Toulouse, 31062
[2]School of Electrical Engineering and Informatics, Bandung Institute of Technology, Jalan Ganesha, 10, Bandung, Indonesia, 40132
[3]PT. PLN (Persero) Jalan Trunojoyo, Blok M I/135, Jakarta, Indonesia, 12160
[4]Electric Power Unversity, 235 Hoang Quoc Viet, Hanoi, Vietnam
[*]Email: nugroho.at@gmail.com

***Abstract*—The electric field distribution in polymer dielectric under DC stress is temperature and time dependent and it can be determined by using conductivity which is also dependent on field and temperature. The distribution of the field, that directly impacts the cable performances, is driven by the conduction mechanisms and settles with giving rise to a space charge distribution across the insulation. To predict conductivity-related electric field distributions, conduction current measurement under various electrical and thermal conditions in time need to be recorded. The current measurement is eventually made with polarity reversal in order to relate to the field distribution under this condition. The aim of this paper is to observe and investigate the steady state and transient electric field distribution in miniaturized HVDC power cables with construction of 1.5 mm cross-linked polyethylene (XLPE) insulation thickness. The determination of field distribution is achieved by computation using current-voltage model for current transient in cable geometry approach. Both isothermal and thermal gradient conditions for the cable are analyzed, as a function of stressing time and applied voltage. The most critical stresses for the model cases are identified.**

Keywords— Conductivity, HVDC cable, electric field distribution, thermal gradient, polarity reversal, space charge.

I. INTRODUCTION

In polymeric solid insulations, when the applied electric field exceeds the space charge accumulation threshold, injected charge from electrodes may be captured by traps distributed in insulation bulk and in this way a space charge builds-up[1][2]. According to the work of McAllister et al[3], the accumulation of charge is considered to be the consequence of a non-uniform electrical conductivity. The effects of temperature and electric field on conductivity are considered in this case. This shows that a space charge can be generated by design into insulations. Indeed, due to this temperature dependence of the conductivity in any insulating material, a temperature gradient generates conductivity gradient, eventually in a steady state charge distribution ρ. Assuming on the temperature dependence of conductivity, by using Maxwell's equation, the electric field distribution in the cable insulation, in cylindrical geometry and under steady state condition is given by [4]:

$$E(r) = E_o \frac{r_o \sigma_o}{r \sigma(r)} \tag{1}$$

where E_o and σ_o are the electric field and conductivity at the reference position r_o. Charge density associated with non-uniform conductivity is of the form:

$$\rho_g = -E(r) \frac{\varepsilon}{\sigma(r)} \frac{\partial \sigma(r)}{dr} \tag{2}$$

where ε is the dielectric permittivity of the material. In the relation to Arrhenius law with activation energy E_a, the charge density can be written according to the following equation:

$$\rho_g = -\varepsilon . E(r) \frac{-E_a}{k_B T^2} \frac{\partial T}{\partial r} \tag{3}$$

where T is the absolute temperature and $k_B = 8.62\ 10^{-5}$ eV/K is the Boltzmann's constant. These expressions show that the space charge profile is controlled by the temperature gradient into the material.

II. EXPERIMENTAL SETUP

A. Test specimen

In this paper, experiments were performed on the same single polymeric DC mini-cables consisting of an inner conductor, an inner semi-conductive layer, the cross-linked polyethylene (XLPE) insulation and an outer semi-conductive layer as depicted in Fig. 1. The mini-cable used in these experiments is with 1.5 mm cross-linked polyethylene (XLPE) insulation thickness.

This scaled down test model of a DC power cable is produced by an extrusion process, the crosslinking process of the whole process producing chemical bond at the semicon-insulation interfaces. The result is a chemical interface

Cite as: N. Adi, G. Teyssedre, T.T.N. Vu, N. Sinisuka, "*DC field distribution in XLPE-insulated DC model cable with polarity reversal and thermal gradient*", IEEE Int. Conf. on High Voltage Engineering and Application (ICHVE), Chengdu, China, 19-22 Sept. 2016. Proc. ICHVE 2016, pp. 1-4, **2016**. DOI: 10.1109/ICHVE.2016.7800612

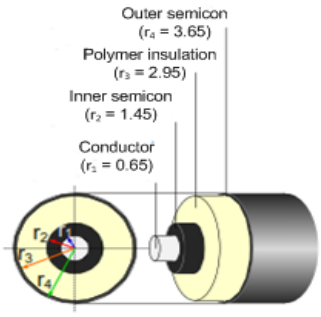

Fig. 1: Schematic representation of DC mini-cable

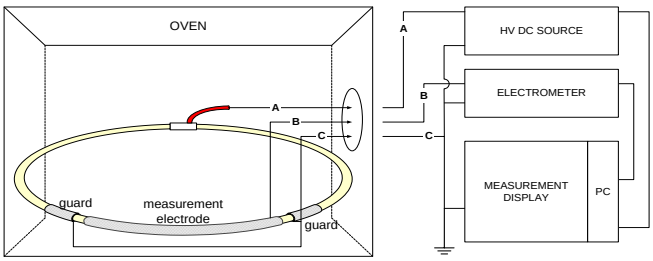

Fig. 2: Conduction current measurement setup

between the insulation and the semicon in the mini-cable which is similar to those found in a full scale DC power cable. With this reduced dimension, the cost of production, transportation and testing of these cables is substantially reduced.

B. Conduction current measurement on mini cable sample

Fig. 2 shows a schematic of the setup of the conduction current measurement in the mini-cable. The sample was peeled off by removing the outer SC layer for preventing surface conduction. The guard sections are prepared with 20 mm length at both ends of the measurement area and 20 mm apart from the measurement section of 250 mm length. The 1m-long specimen was installed as a ring inside the oven where both the end parts of the cable are jointed and connected to 35 kV DC high voltage generator from FuG Elektronik GmbH. The measurement and guard sections are connected to a Keithley 617 electrometer through a protecting circuit and the results are displayed in the PC screen monitor.

Measurements were performed under different temperatures varying from 30 °C to 90 °C by step of 10 °C. For each of the temperature levels, charging/discharging current measurement were realized for 11 values of applied voltage ranging between 2 and 30 kV under isothermal conditions with polarization/depolarization steps last for 1h/1h.

III. RESULTS AND DISCUSSION

A. Conductivity measurement

Fig. 3 shows the results of conduction current measurement as a function of field at various levels of temperature applied. The presented data correspond to charging current measurement after 1-hour polarization time.

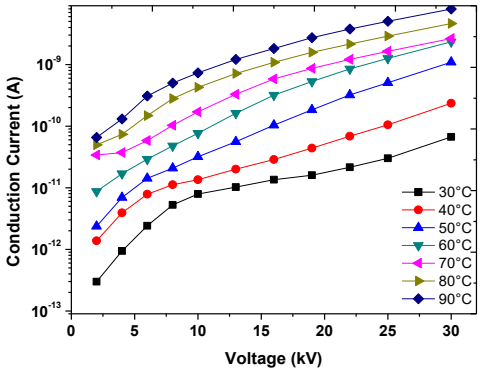

Fig. 3: Conduction current results as a function of field at various temperatures

We can see that the conduction currents are strongly dependent on field and temperature as the magnitudes are rising following the increase of temperature and field. The current values range from 0.3 pA at the lowest field and temperature (2 kV / 30 °C) to 8 nA at the highest field and temperature (30 kV / 90 °C).

Regarding to the strong field and temperature dependency of the conduction currents characteristics, an analytical expression of conductivity with temperature and electric field following semi-empirical equation has been used to fit the experimental data:

$$\sigma(E,T) = A \cdot \exp\left(\frac{-E_a}{k_B T}\right) \cdot \frac{\sinh\left(C(T) \cdot E(r)\right)}{E(r)} \tag{4}$$

In order to simplify the expression, we can note that,

$$B = A \cdot \exp\left(\frac{-E_a}{k_B T}\right) \tag{5}$$

Equation (4) can be rewritten by:

$$\sigma(E,T) = B \frac{\sinh\left(C(T) \cdot E(r)\right)}{E(r)} \tag{6}$$

So the current flowing in the outer circuit during steady state period at given temperature can be written as:

$$I(T) = B.\sinh\left(C(T).E(r)\right).2\pi.r.l \tag{7}$$

From the equation above we can obtain the expression to determine the electric field at the radius r as follows:

$$E(r) = \frac{1}{C} \cdot \sinh^{-1}\left(\frac{I}{B \cdot 2\pi r \cdot l}\right) \tag{8}$$

In order to determine the conductivity expression of Eq. (4), we first estimated B and C values for measurements at a single temperature by optimization, considering experimental quasi steady state charging currents-voltage. However, the relation between current and field cannot be applied directly as would be the case of flat geometry since the field distribution depends on the expected conductivity expression. To solve the problem we proceeded by integrating the electric field E(r) in

Cite as: N. Adi, G. Teyssedre, T.T.N. Vu, N. Sinisuka, "*DC field distribution in XLPE-insulated DC model cable with polarity reversal and thermal gradient*", IEEE Int. Conf. on High Voltage Engineering and Application (ICHVE), Chengdu, China, 19-22 Sept. 2016. Proc. ICHVE 2016, pp. 1-4, **2016**. DOI: 10.1109/ICHVE.2016.7800612

Eq. (8) from the inner to outter radius which gives the relationship between the applied voltage (V_{app}) and the conduction current (quasi steady state current) as follows [5]:

$$-V_{app} = \frac{M(I)}{C}\left(\frac{\sinh^{-1}(M_I)}{M_I} - \frac{\sinh^{-1}(M_O)}{M_O} + \frac{1}{2}\cdot\log 10\left\{\frac{\left[M_O^{\,2}+1\right]^{0.5}-1}{\left[M_O^{\,2}+1\right]^{0.5}+1}\right\}\cdot\left\{\frac{\left[M_I^{\,2}+1\right]^{0.5}+1}{\left[M_I^{\,2}+1\right]^{0.5}-1}\right\}\right) \quad (9)$$

where

$$M(I) = \frac{I}{B\cdot 2\pi\cdot l}, M_I(I) = \frac{I}{B\cdot 2\pi\cdot l\cdot r_i}, M_O(I) = \frac{I}{B\cdot 2\pi\cdot l\cdot r_O}$$

Table 1 provides the conductivity model parameters. From B(T) and C(T) obtained through optimization, we first deduced the values of A constant and thermal energy activation, E_a by using Arrhenius fit to B×C product plot considering that at sufficiently low field the conductivity is approximated by: σ(T)= B(T)×C(T). As C did not appear significantly temperature dependent, we considered a constant value.

Fig. 4 shows the conductivity vs. E and T obtained by voltage-current model. We can see that a threshold like behaviour comes out from the representation, with a threshold field independent of temperature, which is $E_t \approx 11.5$ kV/mm. The relation to the value of C, which actually controls the threshold, can be deduced as $E_t \approx 2.5/C$. Below the threshold, the response tends to follow Ohm's law which means conductivity independent from field. But as the field is increasing, it begins to be a non-linear relation. The reason can be space charge effects that accumulate at high fields through e.g. space charge limited current. An alternative would be to have a hopping conduction with mobility dependent on field as temperature/field is rising. The two processes may have different temperature dependence of the threshold. With the assumption of using best average C constant value, we cannot reveal this feature in the modelled temperature dependent conductivity characteristic.

Fig. 5 shows the comparison between measurement results and model. Compared to the measurement result, the model gives a fairly good fit of the current vs. field plot as shown in Fig. 5. It implies that the expression model in Eq. (4) is validated as an appropriate model to the data available here.

B. Electric field simulation based on conductivity data

We have followed the route consisting in using the conductivity model as input to finite element modelling of the field distribution in cables under thermal gradient [6]. Such approach was applied on Medium Voltage cables to estimate space charge and field profiles as a function of time [6] and also to deduce the shape of the transient current in case of mini-cables [5].

TABLE 1 THE PARAMETERS OF CONDUCTIVITY MODEL

Parameter	Value
C (m/V)	2.15 x 10^{-7}
A (S.V/m^2)	3.83 x 10^4
Ea (eV)	0.828

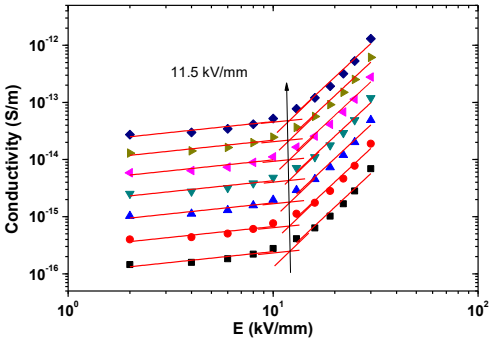

Fig. 4: Conductivity fit from computation

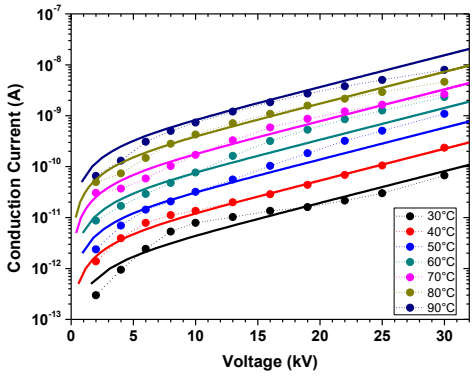

Fig. 5: Fit model (solid line) and conduction current data (circle)

The first simulation set was run at voltage applied of 15 kV, with polarization time of 2 hours and 10 °C of thermal gradient is applied across the insulation at the mean temperature of 65 °C. The conductor temperature is 70 °C and outer temperature of insulation 60 °C. The field profiles of Fig. 6 shows decreasing trends near the conductor and increasing at the outer part of insulation. At the first 100 s, the maximum field is laid at the inner semicon-insulation interface, being 13.5 kV/mm, while the minimum field is at the insulation- outer semicon interface and is 7.4 kV/mm. As the time is rising, there is field redistribution in the insulation due to the gradient in conductivity induced by the thermal gradient. The field near the conductor tends to decrease following the polarization time whereas the field at the outer interface of insulation-semicon begins to increase. At the end of polarization, the field inversion is shown where the field near the conductor has dropped to 9.8 kV/mm which is lower than that at the outer insulation where the magnitude reached over 10 kV/mm.

We consider next the case of polarity reversal simulation in isothermal condition at temperature of 65 °C, considering there is no load operating in the cable. Fig. 7 shows the simulation result of electric field profiles with polarization time of 2 hours and voltage polarity inversion applied of -15 kV, inversed after 2 hours positive polarity polarization time. The field profile across the insulation thickness does change

Cite as: N. Adi, G. Teyssedre, T.T.N. Vu, N. Sinisuka, "*DC field distribution in XLPE-insulated DC model cable with polarity reversal and thermal gradient*", IEEE Int. Conf. on High Voltage Engineering and Application (ICHVE), Chengdu, China, 19-22 Sept. 2016. Proc. ICHVE 2016, pp. 1-4, **2016**. DOI: 10.1109/ICHVE.2016.7800612

reasonably along 2 hours polarization time. The effect is only due to the non-linear conductivity with field, which tends to homogenize the field in the insulation. This profile is similar to the Laplacian-field profile (considering at t = 0 s).

Comparing to the positive polarity steps, the field profile at the inversion step is slightly higher. This is due to the residual field built up under the positive step. We can see in Fig. 7 that the field magnitude at the inner semicon at -15 kV after 300 s of voltage inversion, that is 15.1 kV/mm is higher than the same period in the positive steps that is 13.4 kV/mm.

Fig. 8 shows the simulation results of electric field profile at ±15 kV voltage polarity inversion applied with 10 °C thermal gradient and 2 hours polarization time. The mean temperature is set to 65 °C. The voltage polarity inversion does make the field profile at the negative step is higher than at the positive step, both at the inner and the outer semicon-insulation interface. Its magnitude difference is equal to the residual field after the polarization step.

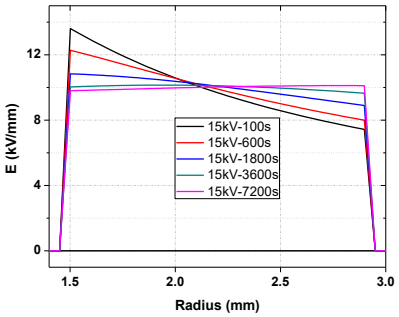

Fig. 6: Field distribution profile in sample cable with T gradient = 10˚C at voltage applied of 15 kV

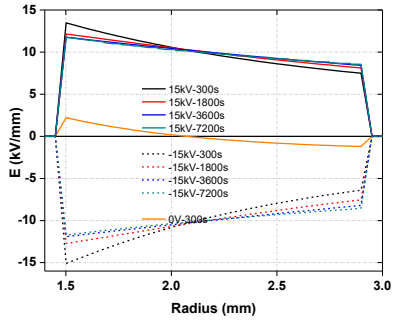

Fig. 7: Field distribution profile in cable sample under voltage inversion applied and at isotherm condition at T=65°C.

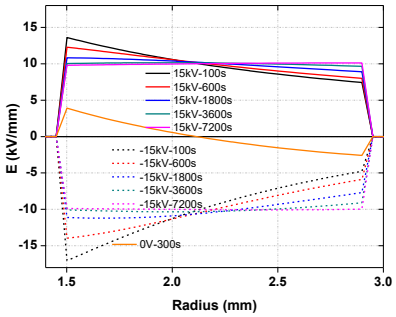

Fig. 8: Field distribution profile in sample cable with voltage inversion applied of ±15 kV and at T gradient = 10˚C.

When thermal gradient is applied across the insulation, while current homogenization in the insulation takes place and space charge settles, the field profile at the inner semicon decreases and increases at the outer semicon. This phenomenon of field inversion is the same as the one occurred in the first simulation, but with the influence of voltage polarity inversion, the inversion of field seems higher than at isotherm condition. The field at the inner semicon is decrease from 17 kV/mm to 9.9 kV/mm and at the outer semicon is increase from 4.7 kV/mm to 9.9 kV/mm.

IV. CONCLUSION

The field distribution within the insulation of cables under thermal gradient and polarity inversion can be obtained through simulation based on conductivity characteristics from the measurement. Owing to the field grading nature of the material the field distribution in isothermal conditions is homogenized in respect to the capacitive field distribution. The conductivity gradient under thermal gradient applied combined to the non-linearity in field leads to very good homogenization of the field in the insulation for voltage of 15 kV. Electric field distribution is higher at the insulation-outer semicon interface than at conductor semicon-insulation interface under thermal gradient simulation. Hence, in the polarity inversion stage, electric field at the inner semicon is strongly enhanced, by about 30% of the capacitive field and 100% of the steady state field.

ACKNOWLEDGMENT

We acknowledge PLN for the financial support during research stay of N. Adi in Laplace Laboratory, University Paul Sabatier, Toulouse III, France.

REFERENCES

[1] G.C. Montanari, “The electrical degradation threshold of polyethylene investigated by space charge and conduction current measurements,” IEEE Trans. Dielectr. Electr. Insul, vol. 7, pp. 309–315, 2000.

[2] L.A. Dissado, C. Laurent, G.C. Montanari, and P.H.F. Morshuis, “Demonstrating a threshold for trapped space charge accumulation in solid dielectrics under DC field,” IEEE Trans. Dielectr. Electr. Insul., vol. 12, pp. 612–620, 2005.

[3] I.W. McAllister, G.C. Crichton, and A. Pedersen, “Charge accumulation in DC cables: A macroscopic approach.,” Proc. IEEE Internat. Symp. Electr. Insul., pp. 212–216, 1994.

[4] D. Fabiani, G.C. Montanari, C. Laurent, G. Teyssedre, P.H.F. Morshuis, R. Bodega, and L.A. Dissado, “HVDC Cable Design and Space Charge Accumulation. Part 3: Effect of Temperature Gradient,” IEEE Electr. Insul. Mag., vol. 24, no. 2, pp. 5–14, 2008.

[5] T.T.N. Vu, G. Teyssedre, B. Vissouvanadin, J.Y. Steven, and C. Laurent, “Transient Space Charge Phenomena in HVDC Model Cables,” Proc. 9th International Conference on Insulated Power Cables, pp. 1-6, 2015.

[6] T.T. N.Vu, G. Teyssèdre, B. Vissouvanadin, S. Le Roy, C. Laurent, M. Mammeri, and I. Denizet, “Field distribution in polymeric MV-HVDC model cable under temperature gradient : simulation and space charge measurements,” Eur J. Electr. Engg., vol. 17, 307-325, 2014.

Cite as: N. Adi, G. Teyssedre, T.T.N. Vu, N. Sinisuka, "*DC field distribution in XLPE-insulated DC model cable with polarity reversal and thermal gradient*", IEEE Int. Conf. on High Voltage Engineering and Application (ICHVE), Chengdu, China, 19-22 Sept. 2016. Proc. ICHVE 2016, pp. 1-4, **2016**. DOI: 10.1109/ICHVE.2016.7800612